Approximate Solutions for Nonlinear Gas-Solid Noncatalytic Reactions

Giacomo Cao, Arvind Varma, and William Strieder
Dept. of Chemical Engineering, University of Notre Dame, Notre Dame, IN 46556

In the context of gas-solid noncatalytic reactions, several models have been developed in the literature (for comprehensive reviews, cf. Szekely et al., 1976; Doraiswamy and Sharma, 1984). This work focuses on the sharp-interface model (SIM), which can be used to describe, once incorporated into a suitable reactor model, a variety of chemical and metallurgical processes including the roasting of zinc sulfide (Yoshida and Wen, 1970) and the combustion of coal (Baron et al., 1978). Under the assumptions of isothermal conditions, equimolar counter-diffusion of reacting and product gases and pseudo-steady-state approximation, an analytical relationship that provides the time required to reach the desired conversion of a single particle of the solid reactant can be derived in a straightforward manner for the case of a first-order reaction with respect to the gaseous reactant (Szekely et al., 1976). The assumption of a first-order reaction, however, can be valid only over a limited range of conditions and may not even be true when the gaseous reactant is adsorbed strongly on the solid surface. A number of examples of nonlinear gas-solid noncatalytic reactions are reported in the literature (Cannon and Denbigh, 1957; Habashi, 1969; Chu and Rahmel, 1979). For nonlinear kinetics, the conversion of the solid reactant as a function of time has to be computed numerically, as shown by Sohn and Szekely (1972) for power-law kinetics and by Ramachandran (1982) for Langmuir-Hinshelwood (L-H) kinetics.

Since the analysis for a reactor requires solving the single particle problem repeatedly at every axial and radial position within the reactor, this can be cumbersome if the single particle problem itself has to be solved numerically. Thus, it is of interest to develop good approximate solutions for the case of nonlinear reactions. Several recent publications (Regalbuto et al., 1988, 1989, the references given there) have discussed systematic procedures to obtain good approximate solutions to nonlinear diffusion-reaction equations using the Maximum Principle (Protter and Weinberger, 1967). A unique advantage of this technique, not present in alternative methods, is that it provides *rigorous* upper and lower bounds on the true numerical solution. In this work, we extend this method to obtain analytical, and rather tight, upper and lower bounds on the time required to reach any desired solid reactant conversion for nonlinear gas-solid noncatalytic reactions following a SIM, *without* any assumptions about possible rate-controlling regimes. In addition, the analysis allows us to describe some features of the SIM which have previously not been discussed in the literature.

Basic Equations

An isothermal nonlinear noncatalytic reaction occurring in a spherical particle of radius R_o between a gas A and a solid B, according to the following general scheme:

$$\nu_A A_{(g)} + \nu_B B_{(s)} \rightarrow \nu_P P_{(g)} + \nu_s S_{(s)}$$
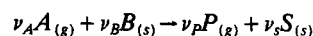
is assumed to take place at a sharp interface between the exhausted outer shell and the unreacted core of the solid, that is, the SIM applies. Under the assumptions of pseudo-steady-state approximation, constant pellet size and equimolal counterdiffusion of gaseous reactants and products, the dimensionless rates of diffusion of the reactant gas through the external film around the particle and through the product layer can be written as follows:

$$\psi_A = (1 - u_s) Bi/Da \tag{1}$$

$$\psi_A = z(u_s - u_i)/[Da(1 - z)]. \tag{2}$$

The dimensionless rate of chemical reaction at the interface can be expressed in the general form:

$$g(u_i) = \psi_A/z^2 \tag{3}$$

where $g(u_i)$ is any monotonically increasing nonlinear function.

The dimensionless material balance for the solid reactant B in terms of movement of the reaction interface, z with all the other quantities as defined in the Notation, is given by:

$$-\frac{dz}{d\tau}=g(u_i) \qquad (4)$$

with initial condition (IC):

$$z=1; \quad \tau=0. \qquad (5)$$

We consider one example of nonlinear kinetics, namely the L-H kinetics:

$$g(u_i)=\frac{(1+\epsilon)u_i}{1+\epsilon u_i}. \qquad (6)$$

The solution of the problem given by coupling Eqs. 1-5 provides the dimensionless position of the reaction interface, z which is related to the solid conversion, X through the equation:

$$X=1-z^3 \qquad (7)$$

as a function of time, τ. Analytical solutions to this problem for τ as a function of z (or X) can be found (Doraiswamy and Sharma, 1984), *only* if $g(u_i)$ is a linear function, when $\epsilon=0$ in Eq. 6.

Analysis of Reaction Behavior

Before proceeding to obtain approximate analytical solutions, it is worthwhile to examine first the structure of the true solution as the reaction evolves in time, starting with zero solid conversion ($z=1$), going eventually to completion ($z=0$). For this, note that coupling Eqs. 1-3 gives:

$$y(z)\equiv Bi\,z-z^2(Bi-1)=\frac{Bi(1-u_i)}{Da\,g(u_i)}\equiv h(u_i) \qquad (8)$$

It is easy to verify that, depending on the value of Bi, $y(z)$ has one of four possible shapes, as shown in Figure 1. The curve of y vs. z is monotone increasing when $Bi\leq2$, while y has an internal maximum, $y_M=0.25\,Bi(1-1/Bi)^{-1}$ at $z_M=0.5\,(1-1/Bi)^{-1}$ for the case of $Bi>2$.

For a given u_i, it is clear from Eq. 8 and Figure 1, that there exists a unique z for $Bi\leq2$. For $Bi>2$, however, if $1\leq h(u_i)<y_M$, there are *two* values of z, given by:

$$z_\pm=\frac{Bi\pm[Bi^2-4(Bi-1)h(u_i)]^{1/2}}{2(Bi-1)}, \qquad (9)$$

a *unique* value of z for $h(u_i)<1$, and *no* real z solution for $h(u_i)>y_M$.

The rate function we are considering, the L-H kinetics, is monotone increasing [$g'(u_i)\geq0$]. For such g, $h'\leq0$: h decreases as u_i increases.

The reaction starts at zero solid conversion, $z=1$ at a value of $u_i=u_{i,0}$ given by the unique solution of $h(u_i)=y(1)\equiv1$, and goes to completion at $z=0$, $u_i=1$ by following the curve $y(z)$. As z varies from 1 to 0, the corresponding value of the interface gas concentration, u_i is obtained by the solution of $h(u_i)=y(z)$. For $Bi\leq2$, it follows then that as the reaction proceeds, u_i increases monotonically from $u_{i,0}$ to 1. For $Bi>2$, however, u_i
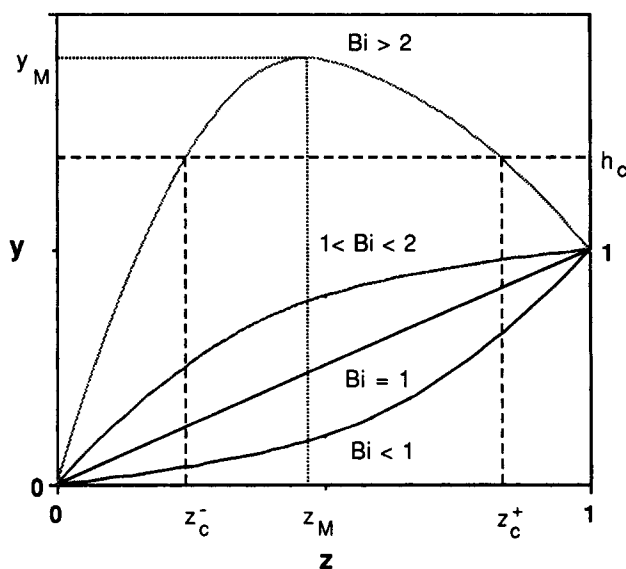

Figure 1. Shape of the curve $y(z)$ for various Bi values.

first decreases from $u_{i,0}$ to its minimum value, u_m at $z=z_M$ and then increases eventually to 1 as z decreases from z_M to 0. *Note that these general considerations are independent of the form of the reaction kinetics g and depend solely on the relative magnitudes of the external and product layer diffusion resistances (Bi).*

The following expressions for $u_{i,0}$ and u_m can be readily obtained for the L-H kinetics:

$$u_{i,0}=[-(\overline{Da}-\epsilon+1)+\sqrt{(\overline{Da}-\epsilon+1)^2+4\epsilon}]/2\epsilon \qquad (10)$$

$$u_m=[-(\overline{Da}y_M-\epsilon+1)+\sqrt{(\overline{Da}y_M-\epsilon+1)^2+4\epsilon}]/2\epsilon \qquad (11)$$

where $\overline{Da}=Da(1+\epsilon)/Bi$. While the above analysis is general and provides a qualitative picture of the reaction process, the quantitative solid conversion X (or z) vs. time, τ behavior can only be obtained numerically for the case of nonlinear kinetics, $g(u_i)$.

One- and Two-Line Upper and Lower Bounds on Reaction Time

As noted earlier, good approximate solutions for nonlinear diffusion-reaction equations can be obtained (Regalbuto et al., 1988, 1989) by using the maximum principle (Protter and Weinberger, 1967). The procedure involves the construction of bounding kinetics made up of line segments so as to generate *upper* and *lower* solutions. The same concept is utilized in this study, although the maximum principle is not applied *per se*.

It can be clearly seen that, if bounding kinetics made up of line segments $g_u(u_i)$ and $g_l(u_i)$ are constructed such that:

$$g_l(u_i)\leq g(u_i)\leq g_u(u_i), \qquad (12)$$

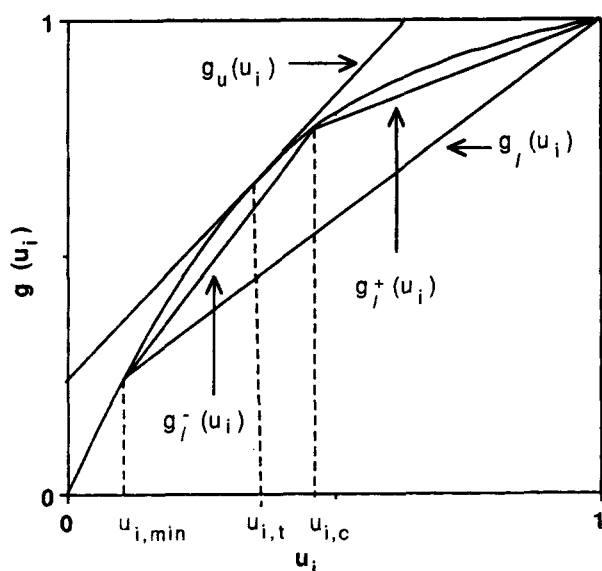then by considering for example the right side of this inequality, from Eq. 4 it follows that:

Figure 2. Reaction kinetics g, one-line upper (g_u) and lower (g_l) bound, and two-line lower ($g_l^- - g_l^+$) bound kinetics.

$$-\frac{dz}{d\tau} = g(u_i) \leq g_u(u_i) \tag{13}$$

which gives:

$$d\tau_l = -\frac{dz}{g_u(u_i)} \leq d\tau \tag{14}$$

whose integration from 1 to z provides a *lower* bound, τ_l on the time, τ required to reach the desired solid conversion, $X = 1 - z^3$. This makes sense, because if $g_u(u_i)$ is used in place of $g(u_i)$ in Eq. 13, then a faster reaction rate will occur, leading to a lower bound on the time to achieve a desired solid conversion, X. Similarly, if $g_l(u_i)$ is used in place of $g(u_i)$ in Eq. 13, a slower reaction rate will occur, leading to an upper bound on time. In summary, then,

$$\tau_l \leq \tau \leq \tau_u. \tag{15}$$

A plot of $g(u_i)$ is shown in Figure 2, together with upper- and lower-bound kinetics considered in the course of this study, which can be constructed in a manner similar to that described elsewhere (Regalbuto et al., 1988). A one-line lower-bound kinetics, $g_l(u_i)$ can be constructed by joining the points $\{u_{i,\min}, g(u_{i,\min})\}$ and $\{1, 1\}$, with $u_{i,\min} = u_{i,0}$ when $Bi \leq 2$ and $u_{i,\min} = u_m$ when $Bi > 2$. Next, an upper-bound kinetics, $g_u(u_i)$, can be

constructed by drawing a straight line tangent to $g(u_i)$ at a point $u_{i,t}$. The procedure for choosing $u_{i,t}$ will be described later.

The bounding kinetics, $g_l(u_i)$ [or $g_u(u_i)$] can then be represented as follows:

$$g_l(u_i) \text{ [or } g_u(u_i)] = (mu_i + b), \tag{16}$$

where expressions for the slopes (m) and intercepts (b) for the one-line upper- and lower-bound kinetics $g_u(u_i)$ and $g_l(u_i)$ are given in Table 1.

Without making any assumptions about possible controlling regimes, an analytical expression for τ can be derived easily when the true kinetics in Eq. 4 is replaced by the linear kinetics given by Eq. 16. This is done by eliminating the u_i dependence through Eqs. 1–2 and 16, and substituting the obtained kinetic expressions into Eq. 4 to give:

$$-\frac{dz}{d\tau} = w(z; m, b)^{-1} \tag{17}$$

where w^{-1} is either g_l or g_u written as functions of z. The subsequent integration leads to:

$$\tau = \frac{m}{m+b} \left[\frac{1}{m} (1-z) + \frac{Da}{2} (1-z^2) \right.$$
$$\left. - \left(1 - \frac{1}{Bi}\right) \frac{Da}{3} (1-z^3) \right]. \tag{18}$$

Some calculations were made using Eq. 18 to determine the time τ required for complete conversion of the solid ($z = 0$ or $X = 1$). The true numerical solution was also obtained by solving the original nonlinear initial value problem, Eqs. 1–6, using standard routines (IMSL Math/Library, 1989). When the one-line upper-bound kinetics, $g_u(u_i)$, consisting of a straight line tangent to the true kinetics at a point $u_{i,t}$ is considered, very tight lower bounds for τ are obtained. For various selected combinations of the dimensionless parameters ϵ, Bi and Da, typical for gas-solid reactions, by varying the tangent point $u_{i,t}$ from $u_{i,\min}$ to 1 with an increment equal to 0.1, using the appropriate parameters m and b from Table 1 and substituting them into Eq. 18, a lower bound on time can be computed. Very small errors relative to the true solution for full conversion ($z = 0$) are found in the entire parameter space and are reported in Table 2 for the specific $u_{i,t}$ values which give the largest lower bound on τ. It can be seen that only for two combinations of parameter values ($Bi = 100$, $Da = 10$, and $\epsilon = 10$ or 100), a relative error greater than 3% is found. It is worth noting that when $\epsilon \geq 10$ and the values of $u_{i,\min}$ are of the order of 10^{-2}, a finer grid around the optimum $u_{i,t}$ value obtained through the 0.1 increment is used to decrease the errors.

Table 1. Slopes and Intercepts for Upper- and Lower-Bound Kinetics

One-line upper-bound:	$m = \dfrac{(1+\epsilon)}{(1+\epsilon u_{i,t})^2}$	$b = \dfrac{(1+\epsilon)\epsilon u_{i,t}^2}{(1+\epsilon u_{i,t})^2}$
One-line lower-bound:	$m = (1 + \epsilon u_{i,\min})^{-1}$	$b = \epsilon u_{i,\min} / (1 + \epsilon u_{i,\min})$
Two-line lower-bound:	$m^- = \dfrac{(1+\epsilon)}{(1+\epsilon u_{i,\min})(1+\epsilon u_{i,c})}$	$b^- = \dfrac{\epsilon(1+\epsilon)u_{i,\min}u_{i,c}}{(1+\epsilon u_{i,\min})(1+\epsilon u_{i,c})}$
	$m^+ = (1 + \epsilon u_{i,c})^{-1}$	$b^+ = \epsilon u_{i,c} / (1 + \epsilon u_{i,c})$

For the one-line lower-bound kinetics $g_l(u_i)$, only for small values of the adsorption parameter ϵ ($\epsilon = 0.1$ and $\epsilon = 1$), Eq. 18 provides acceptable upper bounds within a few percent on the time required to reach complete conversion of the solid for a wide range of Bi and Da numbers. For other values of ϵ, the errors can be large, but are always less than 10%.

These results demonstrate that Eq. 18 provides tight bounds (relative errors less than 3%) on the true numerical solutions when a one-line upper bound kinetics is used. However, the opposite bounds obtained by using one-line lower-bound kinetics are somewhat weaker. These bounds can be improved by drawing two straight-line segments from the points $\{u_{i,\min}, g(u_{i,\min})\}$ and $\{1, 1\}$ that intersect $g(u_i)$ at a point $u_{i,c}$, as shown in Figure 2. The procedure for choosing the point $u_{i,c}$ will be described later; however, each choice of $u_{i,c}$ generates an h_c and z_c, using Eq. 8. The values of the slopes (m) and intercepts (b) for the two-line lower bound kinetics are given in Table 1, and both segments can be represented by Eq. 16. In Figure 2 and Table 1, the negative and the positive superscripts refer to the left- and the righthand segment, respectively.

From the analysis of the reaction behavior discussed previously, it follows that only certain values of $u_{i,c}$ can be selected from Figure 2 as potential points to construct a two-line lower bound on the L-H kinetics. For the case of $Bi \leq 2$, the values of $u_{i,c}$ can be chosen in the range $u_{i,0}$ to 1. From Figure 2, it is clear that when the true kinetics is substituted with the two-line lower-bound kinetics, the lefthand segment relative to $u_{i,c}$ is traced first during the reaction evolution until the value of $u_{i,c}$ is reached. From that time on, the right-hand segment with respect to $u_{i,c}$ has to be considered. When $Bi > 2$, the values of $u_{i,c}$ are selected in the range of u_m to $u_{i,0}$. However, this time when the true kinetics is substituted with the two-line lower-bound kinetics, the right-hand segment with respect to $u_{i,c}$ is traced first during the reaction evolution until the value of $u_{i,c}$ is reached. The intersection of the two line segments with the $g(u_i)$ corresponds to the larger root z_c^+, depicted in Figure 1. The value of u_i goes through a minimum at u_m, now following the lefthand segment and then increases retracing its path until the value of $u_{i,c}$ is reached again. This second intersection with the curve $g(u_i)$ corresponds to the smaller root z_c^-, shown in Figure 1. Finally, the righthand-side segment is traced once again until the reaction goes to completion with $z = 0$ and $u_i = 1$.

The approximate solution for time τ can therefore be obtained for every selected value of $u_{i,c}$, by replacing the true kinetics given in Eq. 4 with the two-line linear kinetics given by Eq. 16 in a manner similar to the one-line bound kinetics. The integration of Eq. 17 has to be performed separately for the two-line lower-bound segments. It follows that:

$$\tau = -\left[\int_1^{z_c} w(z; m^-, b^-)dz + \int_{z_c}^z w(z; m^+, b^+)dz\right];$$
$$Bi \leq 2 \quad (19)$$

$$\tau = -\left[\int_1^{z_c^+} w(z; m^+, b^+)dz + \int_{z_c^+}^{z_c^-} w(z; m^-, b^-)dz\right.$$
$$\left. + \int_{z_c^-}^z w(z; m^+, b^+)dz\right]; \quad Bi > 2 \quad (20)$$

It is apparent that the form of these integrals is the same as that reported in Eq. 18, but the appropriate slopes and intercepts, reported in Table 1, need to be used. Using these expressions, very small errors relative to the true solution for reaction completion time (τ required for $z = 0$) are found in the entire parameter space and are reported in Table 2 for the specific $u_{i,c}$ values, which give the smallest upper bound on τ. It can be seen that the errors never exceed 1.5%.

From Table 2, we can conclude that the relative error with respect to the true solution is always less than 5.4% for the upper-bound and less than 1.5% for the lower-bound kinetics. Hence, using the midpoint estimate, a prediction for the time for complete conversion of the solid can be obtained *analytically* within 3.5%. This accuracy of solution is generally quite acceptable, given the uncertainties involved in evaluating the physicochemical parameters ϵ, Bi, and Da.

Finally, it is worth noting that, although we have treated only the case of Langmuir-Hinshelwood kinetics in this note, similar results can also be obtained for any monotonically increasing nonlinear kinetics $g(u_i)$. For example, in the case of power-law kinetics, relative errors within 3% with respect to the true numerical solution are found when considering two values of the reaction order ($n = 0.5$ and 2), where analytic expressions for both $u_{i,0}$ and u_m can be obtained readily by solving the related quadratic equations.

Table 2. %Error Relative to the True Numerical Solution of Reaction Completion Time for One-Line (δ_1) Upper- and Two-Line (δ_2) Lower-Bound Kinetics

		ϵ							
		0.1		1		10		100	
		δ_1	δ_2	δ_1	δ_2	δ_1	δ_2	δ_1	δ_2
	Da $\downarrow$								
$Bi = 1$	1	0.18	0.08	1.14	0.58	2.25	1.0	0.97	0.6
	10	0.13	0.09	0.68	0.57	1.16	0.84	1.5	0.84
	100	0.07	0.009	0.81	0.05	0.08	0.08	0.94	0.097
$Bi = 10$	1	0.03	0.015	0.13	0.08	0.07	0.04	0.01	0.005
	10	0.1	0.07	0.85	0.5	2.69	1.2	2.71	1.14
	100	0.04	0.014	0.58	0.07	0.06	0.12	0.87	0.13
$Bi = 100$	1	0.04	0.012	0.19	0.06	0.08	0.03	0.01	0.005
	10	0.16	0.086	1.19	0.6	4.0	1.5	5.4	1.29
	100	0.04	0.02	0.54	0.1	0.07	0.16	0.85	0.18

Acknowledgment

Notation

b = intercept of the one-line bound reaction kinetics
b^-, b^+ = intercepts of the two-line bound reaction kinetics g^- and g^+, respectively
Bi = Biot number, $k_g R_0/D_e$
C = gas concentration
D_a = Damköhler number, $R_0 f(C_{Ab})/D_e C_{Ab}$
$\overline{Da}$ = modified Damköhler number, $Da(1+\epsilon)/Bi$
D_e = effective diffusivity of component A
$f(C_{Ai})$ = interface reaction kinetics, $k_i C_{Ai}/(1+K_A C_{Ai})$
$f(C_{Ab})$ = interface reaction kinetics, $k_i C_{Ab}/(1+K_A C_{Ab})$
$g(u_i)$ = dimensionless interface reaction kinetics
k_g = gas-film mass-transfer coefficient
k_i = reaction rate constant
K_A = adsorption equilibrium constant for A
m = slope of the one-line bound reaction kinetics
m^-, m^+ = slopes of the two-line bound reaction kinetics g^- and g^+, respectively
M_B = molecular weight of solid B
R_A = interface reaction rate, $4\pi R_i^2 f(C_{Ai})$
R_{Ab} = $4\pi R_0^2 f(C_{Ab})$
R_i = position of the reaction interface
R_0 = pellet radius
t = time
u = dimensionless gas concentration, C_A/C_{Ab}
X = solid conversion
z = dimensionless position of the reaction interface, R_i/R_0

Greek letters

δ_1, δ_2 = percent error with respect to the true solution for one- and two-line bound kinetics
ϵ = dimensionless adsorption constant, $K_A C_{Ab}$
ν = stoichiometric coefficient
ρ_B = density of the solid B
σ = ν_B/ν_A
τ = dimensionless time, $\sigma f(C_{Ab})M_B t/\rho_B R_0$
ψ_A = dimensionless interface reaction rate, R_A/R_{Ab}

Subscripts

A = gas reactant
b = bulk gas-phase value
B = solid reactant
c = intersection value
i = value at the interface between the ash layer and the unreacted core
l = lower bound
m = minimum value
P = gas product
s = value at the solid external surface
S = solid product
t = tangent value
u = upper bound

Literature Cited

Baron, R. E., J. L. Hodges, and A. F. Sarofim, "Mathematical Model for Predicting Efficiency of Fluidized Bed Steam Generators," *AIChE Symp. Ser.*, **74** (176), 120 (1978).

Cannon, K. J., and K. J. Denbigh, "Studies on Gas-Solid Reactions—I. The Oxidation of Zinc Sulfide," *Chem. Eng. Sci.*, **6**, 15 (1957).

Chu, W. F., and A. Rahmel, "The Kinetics of the Reduction of Chromium Oxide by Hydrogen," *Met. Trans.*, **10B**, 401 (1979).

Habashi, F., *Principles of Extractive Metallurgy*, Vol. I, Gordon and Breach, New York (1969).

Doraiswamy, L. K., and M. M. Sharma, *Heterogeneous Reactions: Analysis, Example, and Reactor Design*, Wiley-Interscience, New York (1984).

IMSL Math/Library, FORTRAN Subroutines for Mathematical Applications (1989).

Protter, M. H., and H. F. Weinberger, *Maximum Principles in Differential Equations*, Prentice-Hall, Englewood Cliffs, NJ (1967).

Ramachandran, P. A., "Analysis of Noncatalytic Reactions following Langmuir-Hinshelwood Kinetics," *Chem. Eng. J.*, **23**, 223 (1982).

Regalbuto, M. C., W. Strieder, and A. Varma, "Approximate Solutions for Nonlinear Diffusion-Reaction Equations from the Maximum Principle," *Chem. Eng. Sci.*, **43**, 513 (1988).

Regalbuto, M. C., W. Strieder, and A. Varma, "Approximate Solutions for Nonlinear Diffusion-Reaction Equations using the Maximum Principle: A Case Involving Multiple Solutions," *Chem. Eng. Sci.*, **44**, 2063 (1989).

Sohn, H. Y., and J. Szekely, "The Effect of Reaction Order in Noncatalytic Gas-Solid Reactions," *Can. J. Chem. Eng.*, **50**, 674 (1972).

Szekely, J., J. W. Evans, and Y. Sohn, *Gas-Solid Reactions*, Academic Press, New York (1976).

Yoshida, K., and C. Y. Wen, "Noncatalytic Solid-Gas Reaction in a Fluidized Bed Reactor," *Chem. Eng. Sci.*, **25**, 1395 (1970).